

# THE 4TH INTERNATIONAL CONFERENCE ON ALUMINUM ALLOYS

## HOT WORKABILITY OF PARTICULATE COMPOSITES WITH VARIOUS Al ALLOY MATRICES

H.J. McQueen<sup>1</sup>, X. Xia<sup>1</sup>, E.V. Konopleva<sup>2</sup>, Q. Qin<sup>1</sup> and P. Sakaris<sup>1</sup>

1. Mech. Engr., Concordia University, Montreal, Canada, H3G 1M8

2. Inst. Solid State Physics, RAS, 142 432, Chernogolovka, Russia

### Abstract

The composites produced by liquid metal mixing had matrices of A356 (Al-Si), 6061 (Al-Mg-Si) and 7075 (Al-Zn-Mg-Cu). The particulates were either SiC or Al<sub>2</sub>O<sub>3</sub> in concentrations of 10-20v%. They were deformed in torsion over the ranges 200 - 550°C and 0.1 to 5 s<sup>-1</sup>. The dependence of flow stress and ductility on temperature and strain rate are presented. The constants for the sinh-Arrhenius constitutive equation are presented and compared. The apparent activation energies for the composites are much higher than those of simple Al alloys (150-180 kJ/mol), being higher for higher particle content. Microscopy shows the distribution of particles, the growth of cracks and the evolution of non-uniform substructures, notably at higher concentrations of particles.

### Introduction

Particulate metal matrix composites (MMC), initially fabricated by liquid metal mixing and DC casting, have considerable commercial promise because they offer high strength and modulus at a moderate price [1,2]. Their deployment in shaped products depends upon mechanical forming [3,4], particularly at high temperatures where the flow stresses  $\sigma$  are reduced and the fracture strain  $\epsilon_f$  is increased. The bulk matrix alloys selected for a range of strengths exhibit good hot workability as a result of dynamic recovery (DRV), which normally produces softer substructures (larger subgrain size  $d$  and less dense, neater walls) at higher  $T$  and lower strain rate  $\dot{\epsilon}$  [5,6]. The reinforcing particles reduce the workability because of the initial high dislocation density, introduced by their difference in thermal expansivity ( $\Delta CTE$ ) from the matrix and by the constraints to plastic flow arising from their relative rigidity [7]. The matrices include medium strength 6061 (Mg<sub>2</sub>Si precipitates), casting alloy A356 strengthened by Si eutectic particles and high strength 7075 ((MgCu)Zn<sub>2</sub> precipitates) [6]. The reinforcements involve both SiC and Al<sub>2</sub>O<sub>3</sub> of about 18  $\mu$ m diameter in concentrations of 10, 15 or 20v% [8-19]. The objective is a preliminary overview of the dependence on  $T$  and  $\dot{\epsilon}$  of strength, ductility and microstructure of composites in Table 1, produced by liquid metal mixing and graciously supplied by Duralcan, San Diego and Alcan, Kingston Laboratories.

### Experiments And Results

The hot deformation was carried out on a hot torsion machine previously described

[8,9,19]. Because of the strain gradient from center to surface and in consistency with Von Mises yielding criterion, the following equations were employed for surface strain and related stresses [9,10,18,19]:

$$\epsilon = (r/\sqrt{3}L) (\text{angular rotation}) \quad \sigma = (\sqrt{3}/2\pi r^3) (\text{torque}) (3+m+n') \quad (1), (2)$$

where,  $r$  (3.17mm) is gage radius,  $L$  (17.5mm) is length,  $m$  ( $d \log (\text{torque})/d \log \dot{\epsilon}$ ) corrects for  $\dot{\epsilon}$  gradient and  $n'$  ( $d\sigma/d\epsilon=0$  at the maximum) corrects for  $\epsilon$  gradient. Some representative stress-strain ( $\sigma$ - $\epsilon$ ) curves are presented in Figure 1. The flow curves at 400°C, 5 s<sup>-1</sup> are somewhat representative of lower T showing high peak stresses  $\sigma_p$  with rapid to medium declines in stress before fracture ( $\epsilon_f \approx 1$ ). For 1.0 s<sup>-1</sup> in Figure 2, the strongest composites have the 7075 matrix [18] and the weakest, the 6061 matrix [9,10] with the A356 [10,11] being intermediate; the higher volume fraction of particulates was stronger with the SiC<sub>p</sub> in reasonable sequence with the Al<sub>2</sub>O<sub>3</sub>. The strengths of the bulk matrix alloys are lower by 25-50%, being about 50, 70 and 100 MPa<sup>-1</sup> for 6061, A356 and 7075 respectively, since 6061 is alloyed with only

Table 1: Chemical Compositions (w + %)

Material	Zn	Mg	Cu	Fe	Si	Mn
10v%Al <sub>2</sub> O <sub>3</sub> /6061	-	1.0	0.3	0.7	0.6	0.15
20v%Al <sub>2</sub> O <sub>3</sub> /6061	-	1.0	0.3	0.7	0.6	0.1
15v%SiC <sub>p</sub> /6061	-	1.0	0.3	0.7	0.6	0.1
15v%SiC <sub>p</sub> /A356	-	0.35	0.2	0.2	7.0	-
10v%Al <sub>2</sub> O <sub>3</sub> /7075	5.98	2.86	1.60	0.1	0.03	-
15v%Al <sub>2</sub> O <sub>3</sub> /7075	5.82	2.75	1.31	0.1	0.03	-

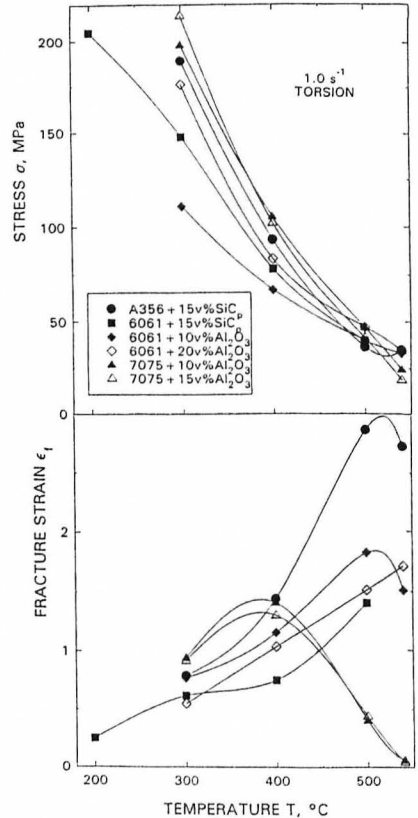
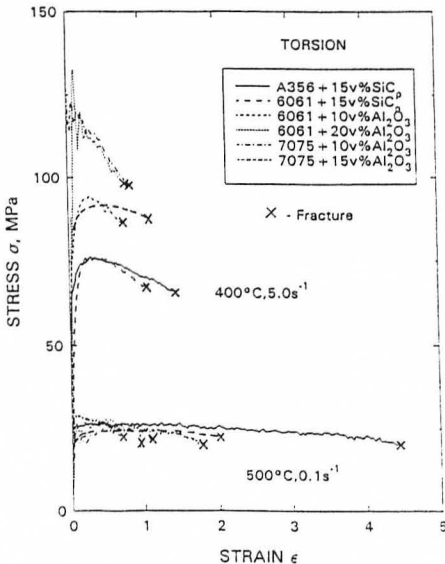


Figure 1. Representative flow curves for all composites tested at 400°C, 5 s<sup>-1</sup> and at 500°C, 0.1 s<sup>-1</sup>.

Figure 2. The variation of maximum  $\sigma$  and  $\epsilon_f$  with T at  $\dot{\epsilon} = 1.0$  s<sup>-1</sup> of A356, 6061 and 7075 MMC with either SiC or Al<sub>2</sub>O<sub>3</sub>.

2% of solute or precipitates, the A356 has 5% eutectic Si particles of about 12  $\mu\text{m}$  average size (almost as large as the SiC particles) and 7075 has 7% of solute and precipitates. At high T (500°C) in Figure 1, the flow curves exhibit medium to long steady state regions with  $\epsilon_f$  ranging from 1 to 4. In the high T regime, the strengths of the composites are only marginally greater than those of the matrix bulk alloys. The strengths at 400°C, 1 s<sup>-1</sup> (Figure 3a) are intermediate between the two extreme behaviours described. The ductilities of the 6061 and A356 increase continuously with rising T, but the ductilities of 7075 composites show a maximum of 1.3 - 1.4.

The dependence of  $\sigma_p$  on  $\dot{\epsilon}$  and T are well represented by the following equation (Figures 3,4) [5,6,9,10,18-21]:

$$A(\sinh \alpha \sigma)^n = \dot{\epsilon} \exp(Q_{HW} / RT) = Z \tag{3}$$

where, R = 8.31 J/molK and  $\alpha = 0.052 \text{ MPa}^{-1}$  as commonly used for Al alloys. The material constants are A, n the stress exponent and  $Q_{HW}$  the activation energy ( $\approx 2.3Rn_{av}s_{av}$ , s slope of log [sinh  $\alpha\sigma$ ] vs. [1/T]). The Zener-Hollomon parameter Z combines the two control variables and can draw all data into a single line as illustrated in Figure 4b. The  $\sigma - \epsilon$  dependence is shown for 400°C in Figure 3a and the Arrhenius  $\sigma - T$  relationship is shown in Figure 3b at 1.0 s<sup>-1</sup> for all the materials. The analysis is illustrated further for A356 composite and alloy; the several constant  $n$  lines in Figure 4a are the best fit by linear regression providing slopes n, which contribute to the average listed in Table 2. The values of  $n_{av}$  (Table 1) fall in the range 2 to 3 without any pattern relative to matrix or particle content. These values cannot be related to the stress exponent in the creep power law, which is about 5 at low  $\dot{\epsilon}$  and  $\sigma$ ; at the present stress levels the power law exponent would be greater than 8. In general, the lines for 500°C are almost always parallel to the 400°C lines but the 300°C lines usually have a higher slope and more scatter; the 7075 MMC's are stronger than the others notably at low T. In the Arrhenius plot (Figure 3b), the slopes are higher for the stronger composites, contributing significantly to the high values of  $Q_{HW}$  (Table 2). The bulk alloys have  $Q_{HW}$  in the range 160-200 kJ/mol, which are higher than for commercial purity Al where 150 kJ/mol can be related to vacancy migration and dislocation climb. The 6061 and A356 composites,  $Q_{HW}$  are in the range 180-260 kJ/mol, in agreement with results of Pickens, Tuler and colleagues [8-10,22,23], whereas 304 and 312 kJ/mol are found for the 7075 composites because of their markedly high strength at 300 and 250°C. The high values of Q reflect the complexity of the dislocation interactions in the composites, which are influenced by the non-uniform constraints from the rigid particles and the high density of

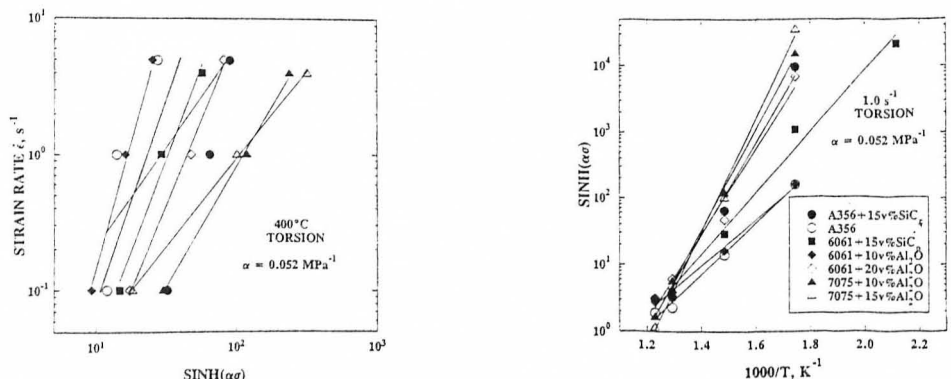


Figure 3. The application of Equation 3 to the data a) variation of  $\sigma$  with  $\dot{\epsilon}$  at 400°C and b) Arrhenius-type dependence of  $\sigma$  upon T at 1 s<sup>-1</sup>.

$\Delta$ CTE dislocations, which have formed due to cooling from solidification [9], thus being independent of the deformation conditions. Industrially, the higher  $Q_{HW}$  indicate that there are more rapid rises in hot strength as T decreases to 300 or 200°C, warning of high finishing forces in forging or rolling [3,4,16].

While the ductilities of the composites rise markedly with climbing T (Figure 2b), they are generally much less than those of wrought bulk alloy. In the case of 6061 MMC,  $\epsilon_f$  increases to approximately 1.5 at 500°C showing no relation to the matrix alloy variation with a maximum of about 18 at 400°C and declines to about 5 at

**Table 2 Constitutive Constants**

Material	n	s	kJ/mol	A (s <sup>-1</sup> )
10v%Al <sub>2</sub> O <sub>3</sub> /6061	2.81	3.35	180	8.5 × 10 <sup>12</sup>
20v%Al <sub>2</sub> O <sub>3</sub> /6061	2.02	6.41	247	1.4 × 10 <sup>15</sup>
15v%SiC <sub>p</sub> /6061	2.7	4.5	233	3.4 × 10 <sup>14</sup>
15v%SiC <sub>p</sub> /A356	3.2	4.3	263	3.6 × 10 <sup>19</sup>
10v%Al <sub>2</sub> O <sub>3</sub> /7075	2.07	7.69	304	1.1 × 10 <sup>19</sup>
15v%Al <sub>2</sub> O <sub>3</sub> /7075	1.95	8.38	312	1.0 × 10 <sup>20</sup>

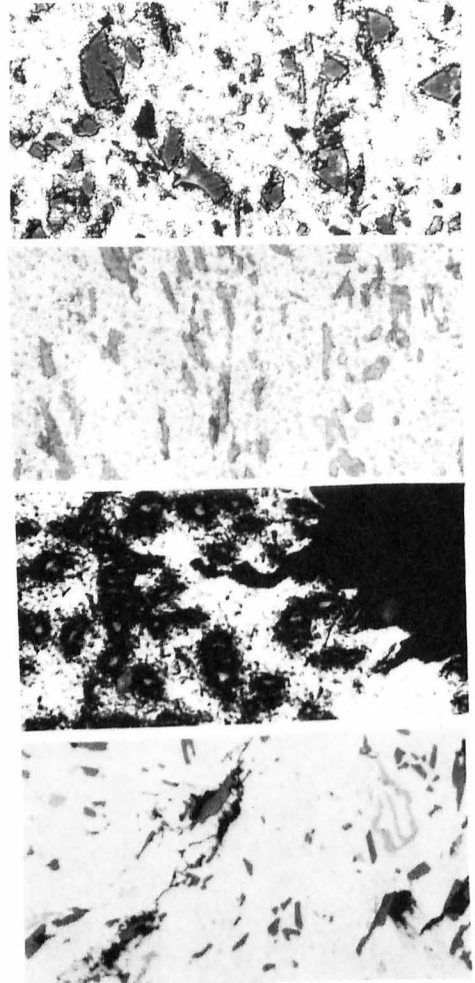


Figure 4. Equation 3 is further illustrated for A356 MMC and matrix: a) constant T lines, approximately parallel and b) Z organizes data into a single line.

Figure 5. Optical micrographs (500°C, 0.1 s<sup>-1</sup>): a)-c) 15v%SiC<sub>p</sub>/ A356, 13μm SiC and 1μm eutectic Si particles and b)-d) A356 bimodal 12μm and 3μm Si particles (X500). Fracture surfaces c) de-cohesion at SiC, ductile tearing at fine Si (X600) d) crack initiation at coarse Si particles, less ductile due to medium Si particles (X400).

500°C [22]. One can reason that the rising level of DRV increases with rising  $T$ , so that the matrix is more capable of blunting the cracks initiated at the particle/matrix interfaces. The mechanism of fracture in bulk worked alloy, i.e. triple junction cracking with rising pore formation at the grain boundary GB, do not come into effect before the composite fails. In the 7075 MMC, there is a maximum at 400°C which exceeds the other composites but then decreases markedly [18]. Bulk 7075 cast alloy exhibits ductility declining from 2.5 to 1.7 from 300 to 400°C (4.5 to 2.7 in a worked alloy); presumably the decline continues as  $T$  rises [24]. At 400°C, the ductility of the matrix does not limit the composite, but above that it probably does. The ductilities of the 6061 and 7075 composites are much less than that of the A356 MMC at about 500°C, where it reaches similar levels as the bulk matrix [10,11]. This could be because the decohesion is more severe in them or their matrices are less capable of restricting propagation; microscopic examination is underway to clarify this.

The specimens which had been rapidly cooled after straining, were polished mechanically for optical examination in an unetched condition to observe the particles and cracks. The plane of section and the slices for TEM were parallel to the torsion axes close to surface. The preparation techniques for TEM and SEM-BSI have been described in detail [12-19]. Because of the similar  $\epsilon_f$  of alloy and MMC, the particle distributions and cracking process in both materials were examined (Figure 5). In the bulk alloy, the large Si particles serve as crack initiators and the medium-sized particles diminish the ductility of the intervening matrix [11,14] so that the ductility is much less than the 6061 alloy discussed above (but somewhat higher than as-cast 7075 at 400°C). In the composite, different solidification conditions lead to very fine Si particles so that they do not act as points of initiation. The failure of the MMC arises from decohesion at particle/matrix interfaces. The increase in DRV with rising  $T$  improves the ability of the alloy to behave in a ductile manner despite the fine particles [11,14].

TEM examination of the 6061 composites with 10v%  $Al_2O_3$ , 15v% Si and 20v%  $Al_2O_3$  revealed that in comparison to the bulk alloy, the dislocation substructure was very inhomogeneous, ranging from uniform distributions to small cells and to subgrains [12-19] (Figures 6,7). The scale of all these distributions shifted to lower densities as  $T$  rose and  $\dot{\epsilon}$  fell. While this behaviour had some similarity to the  $T$  and  $\dot{\epsilon}$  dependence of substructures in bulk alloys, the dislocation distributions were much more inhomogeneous and dense. At 200°C, 1.0 s<sup>-1</sup>, the alloy had an average size of

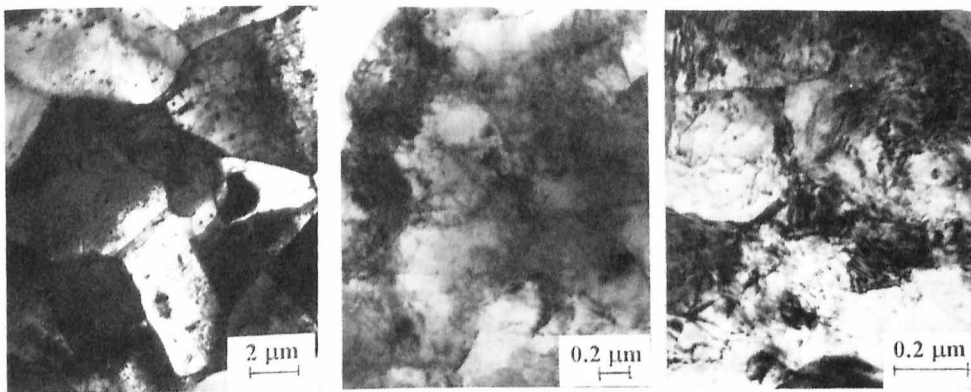


Figure 6. Comparison of TEM substructure developed at 300°C, 1s<sup>-1</sup> in a) 6061 bulk alloy, b) 15v%SiC<sub>p</sub>/6061 and c) 20v%Al<sub>2</sub>O<sub>3</sub>/6061.

1.43  $\mu\text{m}$ , whereas the best recovered group in the 15v% SiC composites had 0.6  $\mu\text{m}$  [16]. At 400°C, 0.1  $\text{s}^{-1}$ , the subgrains are 3.8  $\mu\text{m}$  in the alloy and 1.2  $\mu\text{m}$  in the composite and finally at 500°C, 4 $\text{s}^{-1}$ , 5.6  $\mu\text{m}$  in the alloy and 1.5  $\mu\text{m}$  in the composite. The substructures observed here are much finer and varied than those reported by Chandra and colleagues [25]. For any deformation condition, composites with higher volume fraction of particles had the greatest strength and the highest dislocation density and greatest heterogeneity [12-17,19].

### Discussion

The high dislocation densities are frequently in contact with the particles, since they do not deform and the matrix must undergo additional strain. However, groups of particles set up intense flow patterns, which are between the particles and also accumulate dislocations. In the densest regions, fine cells of 0.1 - 0.2  $\mu\text{m}$  were observed with misorientations of over 20° and are considered to be about to undergo dynamic recrystallization (DRX) (Figure 8) [12-17,19,26]. In other regions, small grains of 0.5 to 2  $\mu\text{m}$  were observed apparently formed by DRX. Because of the evident heterogeneity, DRX did not progress to overrun the entire matrix. One should recall that in DRX, grain growth is stopped by the build up of substructure within the new grains, so that there is insufficient strain energy differential to sustain the migration [26]. There was no evidence of metadynamic recrystallization, that is continued growth of dynamic nuclei after deformation stops. In addition, no static recrystallization was observed.

One may construct the following model of the dislocation distributions as a function of T and  $\dot{\epsilon}$ . In the test samples, there is a high, non-uniform density of  $\Delta\text{CTE}$  dislocations formed during cooling from solidification; there is also a complex distribution of internal stresses [7]. On heating to the deformation T, additional  $\Delta\text{CTE}$  dislocation are generated; this effect is greater for higher T. While being thermally equilibrated at the deformation T, plastic flow relieves the internal stresses higher than the yield stress for that T. There is also static recovery of the substructure which is greater at higher T thus reducing the density more. During deformation, DRV attempts to reduce the dislocation density and develop a substructure consistent with the local strain rate conditions [5,6]. For each particle considered separately, there is a highly localized flow in the adjacent matrix to make up for the absence of flow in the rigid particle. However, the effect of groups of particles must be considered; there are zones of high plastic flow which partially replaces the single particle effects. The DRV produced is highest at the highest T and

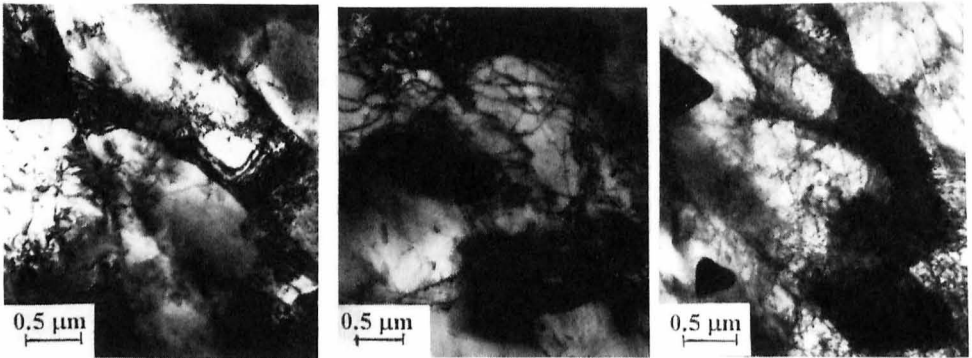


Figure 7. TEM micrographs of 10v%  $\text{Al}_2\text{O}_3/6061$  illustrate decreasing subgrain size with rising  $\dot{\epsilon}$  for 300°C, a) 0.1 $\text{s}^{-1}$ , b) 1 $\text{s}^{-1}$  and c) 5 $\text{s}^{-1}$ .

lowest  $\dot{\epsilon}$ ; moreover, the steady state strain, i.e. where the subgrains are fully developed in the bulk alloy, is about 0.2 (thus there can be considerable reduction in dislocation density during the strain of 2) [5,6]. On cooling to 25°C for observation, more  $\Delta$ CTE dislocations are generated in the specimens from 500°C than from lower T. Low-T slip bands are observed in the highly recovered regions of the 500°C specimens; the additional  $\Delta$ CTE dislocations are not noticeable in low T specimens, e.g. from 300°C, where there already is a high dislocation density.

The above model of the substructure development is able to explain the high activation energies observed in the composites. At high T, the MMC flow stresses are almost the same as those for the bulk alloy because the DRV mechanisms are able to reduce the dislocation densities to about the same level, despite the non-uniform strain distribution imposed by the rigid particles. As T decreases, the initial dislocation density is higher and more heterogeneous. The strain distribution due to the particles tends to become less uniform because of the higher yield stress and localized T increases in the high shear regions. In comparison to the bulk alloy, it becomes more difficult for the DRV mechanisms to rearrange the dislocations into orderly, low energy arrays in association with annihilations: it is to be emphasized that the rates of the unit mechanisms such as climb are not changed, it is just that they do not accomplish as much. In the bulk alloy for any condition, the substructure reaches an equilibrium state related to the flux of dislocations defined by  $\dot{\epsilon}$  and the ability of the unit mechanisms to eliminate and rearrange dislocations [5-6]. In the composites at low T, the equilibrium is never reached, as indicated by absence of a steady state regime. If one used the hypothetical steady state stresses, the activation energy would be much closer to that of pure Al. In age hardenable Al alloys deformed in the solution treated condition, there are increasing levels of dynamic precipitation as T declines leading to very high initial stresses [6]. However as strain progresses, the particles coalesce and recovery is able to reduce the initial high dislocation density to develop a steady state at the same level as material overaged prior to deformation. The activation energies of overaged matrix alloys are similar to that for pure Al [5,6]. The higher stresses at low T in 7075, compared to 6061, may be related to higher levels of precipitation in the former.

### Conclusion

The composites of A356, 6061 and 7075 with 10-20%  $\text{Al}_2\text{O}_3$  or SiC respond well to hot working with marked decrease in flow stresses and increase in ductility, as T increases and  $\dot{\epsilon}$  decreases. The sinh-Arrhenius function provides a suitable definition of the behaviour; however, the apparent activation energies of the

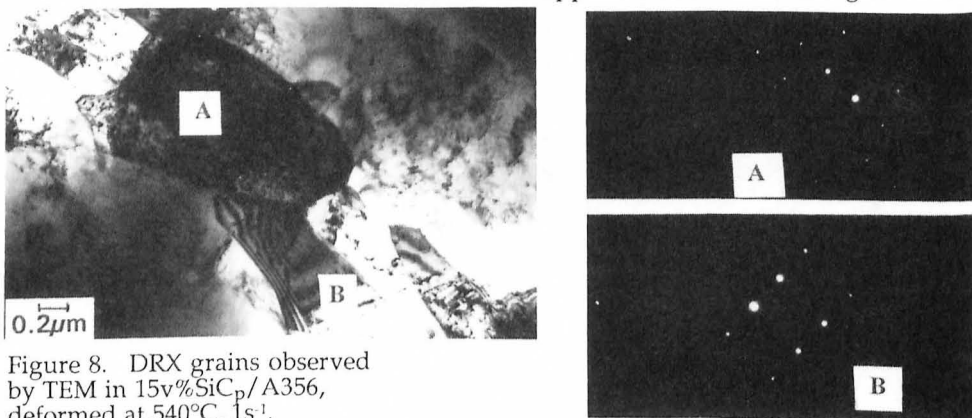


Figure 8. DRX grains observed by TEM in 15v%SiC<sub>p</sub>/A356, deformed at 540°C, 1s<sup>-1</sup>.

composites are very high, ranging upward from 230 kJ/mol in comparison to the range of 150 to 190 kJ/mol for the bulk matrix alloys. The principal mechanism is dynamic recovery, which is much restricted in the composites by the high density of  $\Delta$ CTE dislocations at low T and by the constraints to flow exerted by the rigid reinforcing particles. With rising volume fraction, the particles increase the average density and also the heterogeneity to give a range from subgrains to non-cellular arrays. Unlike the bulk alloys, the dislocation densities in the MMC's rise to such levels that dynamic recrystallization nuclei form near the particles or in regions of concentrated strain. The DRX does not spread throughout the composite.

### References

- 1 D.J. Lloyd, Composite Science and Technology, 35, 159-1791, (1989).
- 2 D.J. Lloyd, Advanced Structural Materials, D.S. Wilkenson, ed., (Pergamon Press, Oxford 1989), pp. 1-21.
- 3 H.J. McQueen and O.C. Celliers, Materials Forum (Australia), 1993, 17, pp. 1-13.
- 4 H.J. McQueen, J. Mat. Proc. Tech., 1993, 37, pp. 3-36.
- 5 H.J. McQueen and K. Conrod, Microstructural Control In Aluminum Alloys, E. H. Chia and H.J. McQueen, eds., (TMS-Aime, Warrendale, PA, 1986), pp. 197-219.
- 6 H.J. McQueen, Hot Deformation of Aluminum Alloys, T.G. Langdon and H.D. Merchant, eds., (TMS-AIME, Warrendale, PA, 1991), pp. 31-54 and 105-120.
- 7 R.J. Arsenault, Strength of Metals and Alloys, (ICSMA9, Tel-Aviv), D.G. Brandon et al., eds., (Freund Pub. Co. Ltd., London, U.K., 1990), 2, pp. 31-46.
- 8 H.J. McQueen and P. Sakaris, Composite Structures and Materials, S. Hoa and R. Gauvin, eds., (Elsevier Applied Science, London, 1992), pp. 297-306.
- 9 P. Sakaris and H.J. McQueen, Aluminum Alloys: Their Physical and Mechanical Properties - Proceedings ICAA3, L. Arnberg, E. Nes, O. Lohne, N. Ryum, eds., (NTH-Sinteff, Trondheim, Norway, 1992), Vol. 1, pp. 554-559.
- 10 P. Sakaris and H.J. McQueen, Advances in Production and Fabrication of Light Metals, (Edmonton), M.M. Avedesian et al. eds., (CIM Montreal, 1992), pp. 605-617.
- 11 H.J. McQueen, P. Sakaris and J. Bowles, Advance Composites 93, (Australia), T. Chandra, A.K. Dhingra, eds., (TMS-AIME, Warrendale, PA, 1993), pp. 1193-1198.
- 12 X. Xia, P. Sakaris and H.J. McQueen, Proc. Ninth Intl. Conf. on Composite Materials, (ICCM/9), Madrid, pp. 157-162.
- 13 X. Xia, H.J. McQueen and P. Sakaris, Developments and Applications of New Ceramics and Metal Alloys, R.A.L. Drew, ed., (CIMM, Montreal, 1993), pp. 135-142.
- 14 H.J. McQueen, E.V. Konopleva and M. Myshlyaev, Proc. 10th Intl. Conf., Strength of Materials, H. Oikawa et al., eds., Japan Inst. Metals, 1994. (In press.)
- 15 X. Xia, and H.J. McQueen, Microstructural Science, (Intl. Met. Soc. Conf., Montreal, 1994). (In press.)
- 16 H.J. McQueen, X. Xia, P. Sakaris, Proc. Intl. Conf. Design and Mfg. Using Composites, (ATMAM '94, Montreal), S.V. Hoa et al., eds., (Montreal, 1994). (In press.)
- 17 X. Xia, P. Sakaris and H.J. McQueen, Proc. Intl. Sym. Light Metals, (Toronto, 1994), Met. Soc. CIMM, Montreal, (1994). (In press.)
- 18 Q. Qin, H.J. McQueen, and J.J. Jonas, Reference [17]. (In press.)
- 19 X. Xia, P. Sakaris and H.J. McQueen, Mat. Sci. Eng., 1994. (In press.)
- 20 P. Sakaris and H.J. McQueen, Reference [9], Vol. 2, pp. 276-281.
- 21 H.J. McQueen and P. Sakaris, Reference [9], Vol. 2, pp. 179-184.
- 22 J.R. Pickens, et al., Metal. Trans., 18A, (1987), pp. 303-312, .
- 23 C. Demetry, J.T. Beale and F.R. Tuler, Advanced Structural Materials, D.S. Wilkenson, ed., (Pergamon Press, Oxford 1989), pp. 33-39.
- 24 E. Evangelista, E. DiRusso, H.J. McQueen and P. Mengucci, Homogenization and Annealing of Al and Cu Alloys, H.D. Merchant et al. eds., (TMS-Aime, Warrendale, PA, 1988), pp. 91-104.
- 25 D. Yu and T. Chandra, Reference [11], pp. 1073-1077.
- 26 H.J. McQueen, E. Evangelista and N.D. Ryan, Recrystallization '90 (Intl. Conf. Recrystallization in Metallic Materials), T. Chandra, ed., (TMS-AIME, Warrendale, PA., 1990), pp. 89-100.